# Applications of electron channelling contrast imaging for characterising nitride semiconductor thin films in a scanning electron microscope


G. Naresh-Kumar[1]*, P. R. Edwards[1], B. Hourahine[1], S. Kraeusel[1], C. Mauder[2], M. Heuken[2], A. P. Day[3], A. Winkelmann[4], P. J. Parbrook[5], A. J. Wilkinson[6] and C. Trager-Cowan[1]

1. Dept. of Physics, SUPA, University of Strathclyde, G4 0NG Glasgow, Scotland, UK
2. AIXTRON SE, Kaiserstr. 98, 52134 Herzogenrath, Germany
3. Aunt Daisy Scientific Ltd, Claremont House, High St, Lydney, Gloucestershire, GL15 5DX, UK
4. Max-Planck-Institut fur Mikrostrukturphysik, 06120 Halle, Germany
5. University College Cork, "Lee Maltings", Cork, Ireland
6. Department of Materials, University of Oxford, Oxford OX1 3PH, UK
*naresh.gunasekar@strath.ac.uk


## Motivation

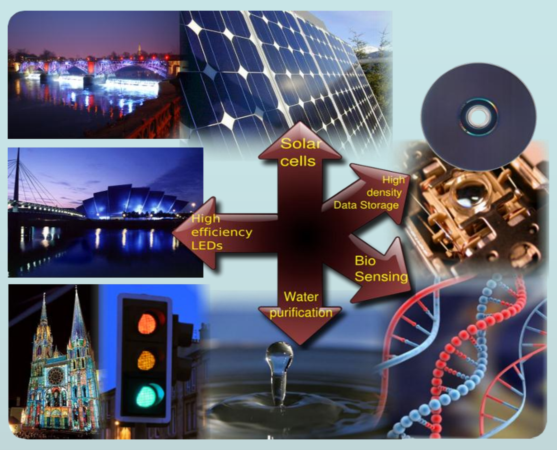

Some of the present and future applications of nitride semiconductors

❖Extended defects such as threading dislocations (TDs), stacking faults (SFs) and partial dislocations (PDs) in nitride semiconductors act as scattering centres for light and charge carriers and thus severely limiting the performances of electronic and optoelectronic devices [1].

❖Developing the capability to analyse extended defects and determine their types and densities rapidly, with negligible sample preparation and without damaging the material under investigation, represents a significant step forward for the development of high quality material and will accelerate the production of new devices.

❖Using electron channelling contrast imaging (ECCI), coupled with the acquisition of electron channelling patterns (ECP) in a scanning electron microscope (SEM), provides such a capability.

## Demonstrating electron channelling in a SEM

**Origin of electron channelling contrast**

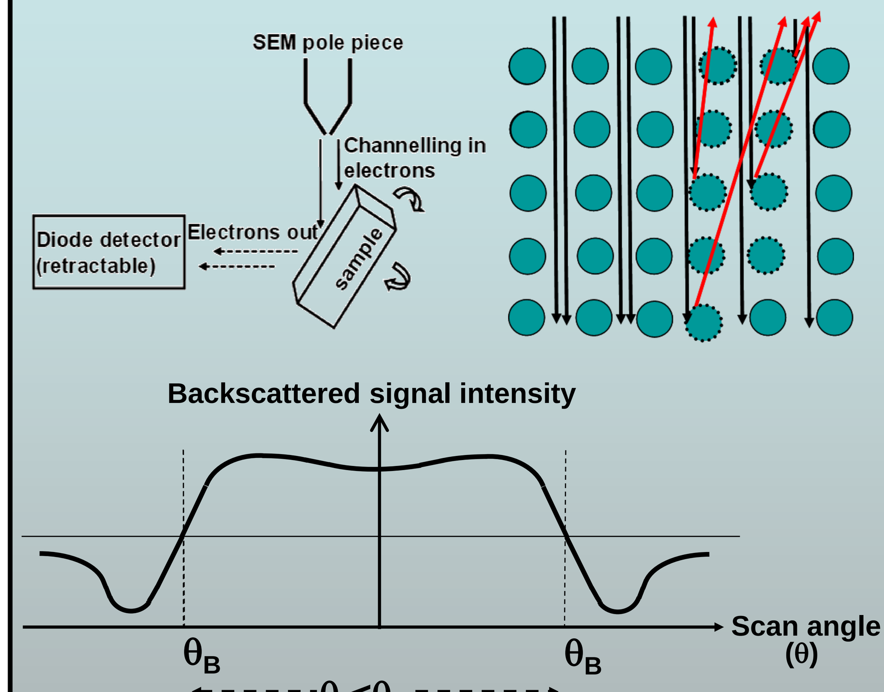


**❖Spatial and depth resolution of tens of nanometres**

**❖In ECCI TDs appear as spots with black-white (B-W) contrast** [2].

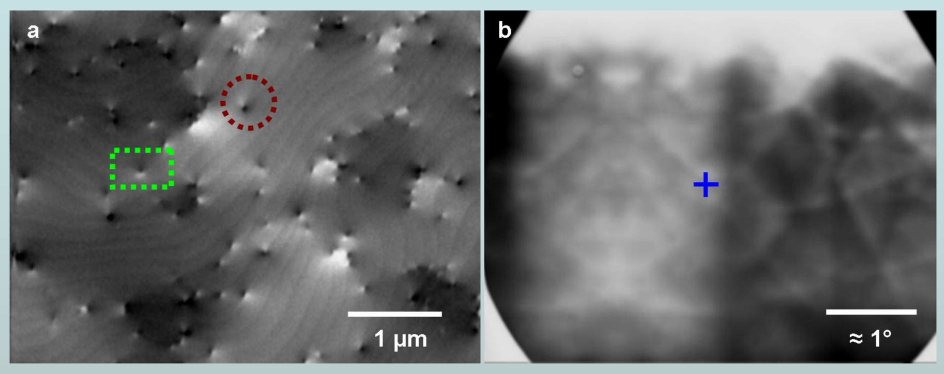


**(a) Multibeam ECCI showing TDs, atomic steps and (b) ECP, both acquired at 30 keV**

❖The dotted circle highlights a dislocation with a screw component and the dotted rectangle highlights an edge dislocation. The cross on the ECP marks the Pattern centre (PC).

## Identifying dislocation types in c- plane GaN using electron channelling

❖Identification of individual dislocation types is necessary to understand the role of TDs on device performance.

❖In many cases pure screw dislocations are the most detrimental to device performance, thus differentiating between pure screw and mixed dislocations becomes important [3, 4].

**❖ECP gives crystal orientation from which crystal planes can be indexed.**

**❖Kinematical simulations are used for indexing**

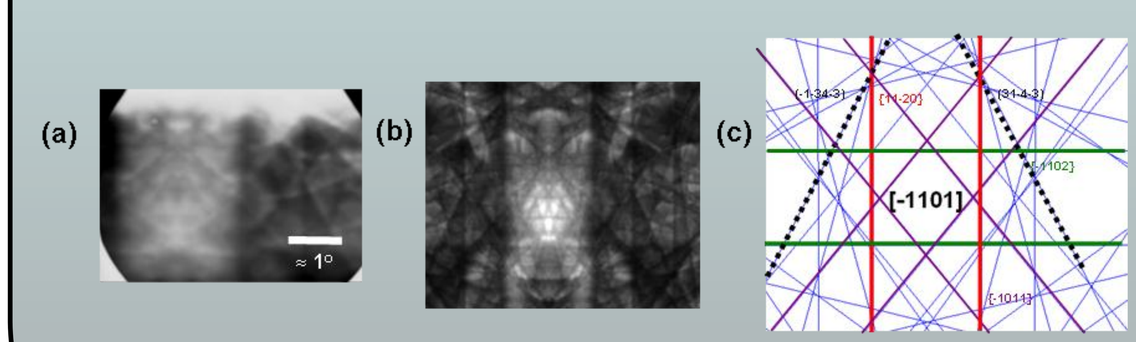


**(a) Experimental ECP, (b) Dynamical simulation of ECP and (c) kinematical simulation of ECP for incident electron beam energy of 30 keV)**

**❖ By choosing an appropriate crystal plane for channelling and from the direction of the B-W contrast, TD types can be identified** [5].

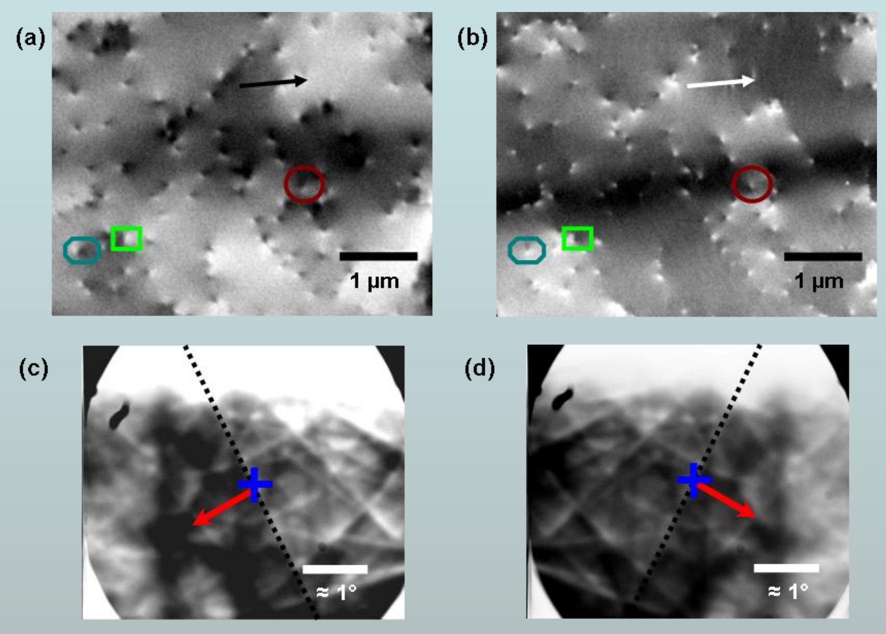


**Two-beam ECCI and ECP revealing dislocation types: (a) & (b) ECCI from the same part of the sample acquired at g of (31-4-3) and (-1-34-3), respectively. (c) & (d) ECPs which correspond to the ECCI shown in (a) & (b)**

❖The circle indicates a screw dislocation, the rectangle an edge dislocation, and the octagon a mixed dislocation. The black and white arrows highlight the change of contrast for sub grains when *g* is changed. The cross shows the position of the PC, the black dotted lines highlight the diffracting planes and the red arrow shows the direction of *g*.

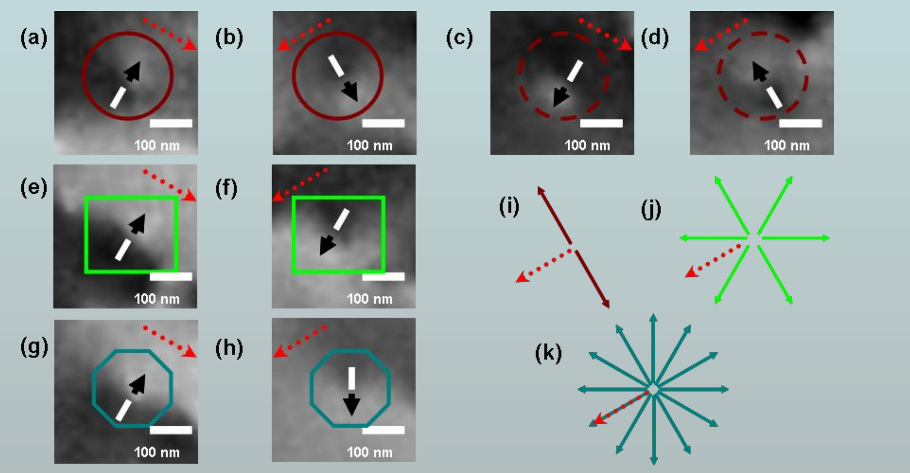


**B-W contrast directions for screw (a-d), edge (e-f) and mixed (g-h) TDs and possible directions of the B-W contrast of screw (i), edge (j) and mixed dislocations (k) for a g of (3 1-4-3). The dotted red arrow denotes the direction of *g***

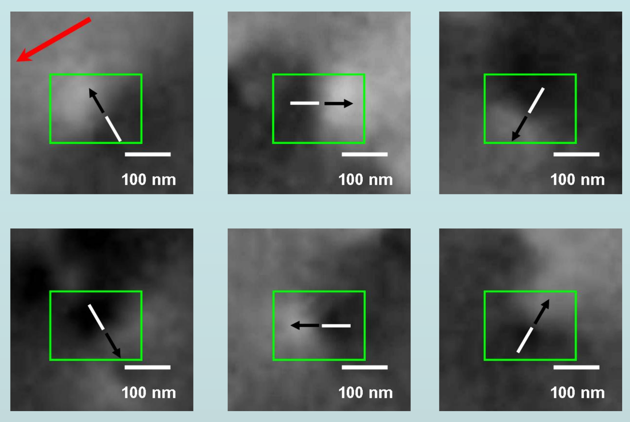


**Six B-W contrast directions of edge dislocations for a *g* of (31-4-3)**

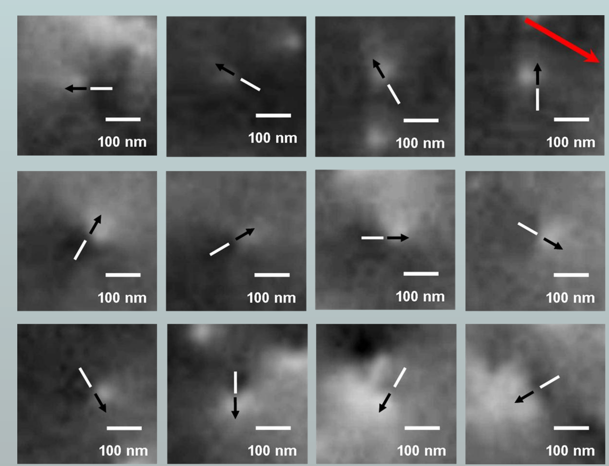


**Twelve B-W contrast directions of mixed dislocations for a *g* of (-1-34-3)**

## Imaging stacking faults and partial dislocations in non-polar (m-plane) nitrides

**Sample structure**

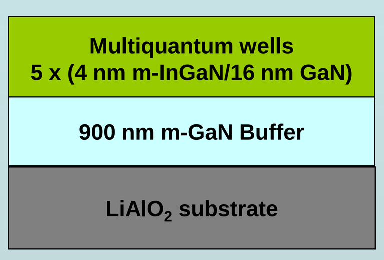


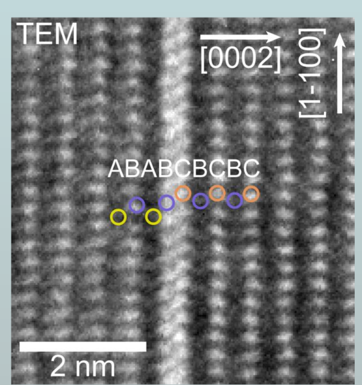


**High resolution cross-section TEM image showing the stacking mismatch**

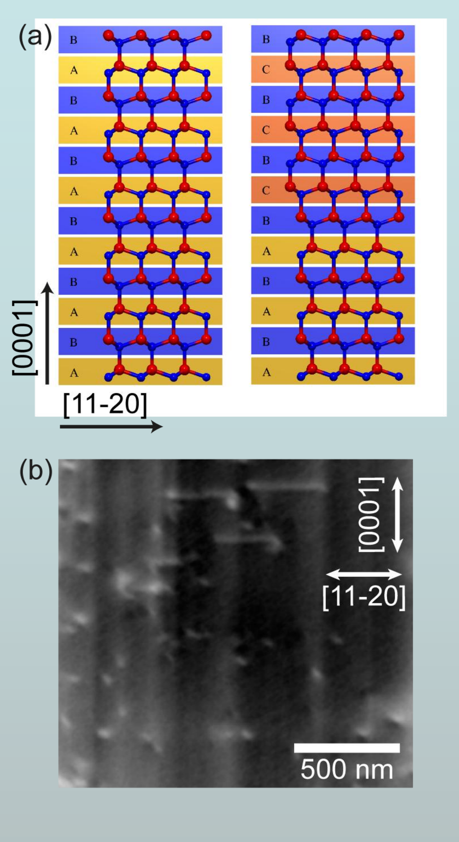


**(a) Schematic diagram of a perfect wurtzite lattice and a basal plane stacking fault of type $I_1$ introduced by replacing the bilayer A (yellow color) to C (red color). (b) ECCI of m-plane GaN buffer layer before growing the MQWs exhibiting BSFs and TDs.**

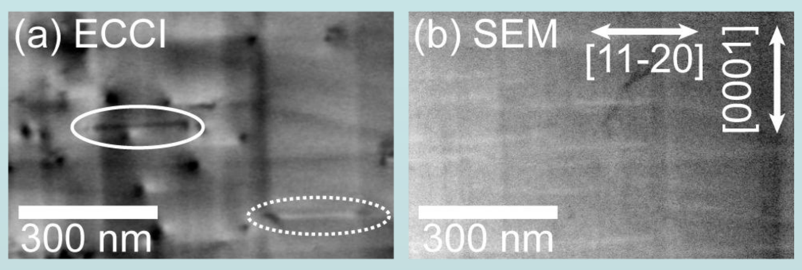


**(a) High magnification ECCI of $In_{0.04}Ga_{0.96}N$/GaN MQW, (b) secondary electron image of the same area.**

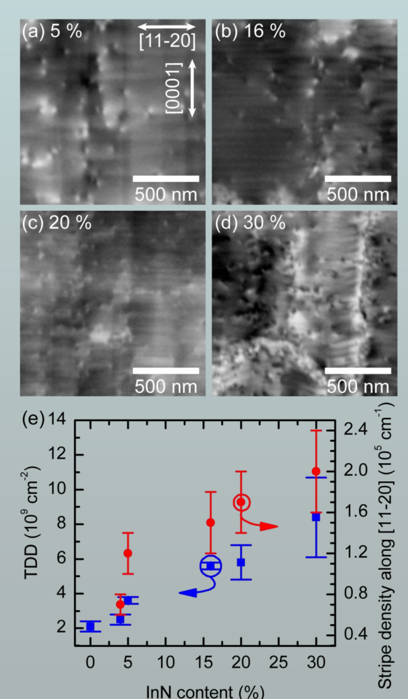


**ECCI showing TDs with MQWs with varying InN%**

## Summary

❖It was demonstrated that ECCI is an ideal technique for rapid and non-destructive quantification of TD and SF densities in nitride semiconductors when compared to the presently available techniques.

❖For the c-plane GaN sample, the total TD density was estimated to be $3.6\pm0.2\times10^8 cm^{-2}$ with pure screw of 7% followed by 42% of mixed and 51% of edge dislocations.

❖For the m-plane GaN buffer layer, the TD density was estimated to be $2.1\pm0.3\times10^9 cm^{-2}$ and assuming the BSFs propagate through the entire sample; their densities were estimated to be $\approx 0.6\times10^4 cm^{-1}$.

❖In order to increase the reliability of ECCI analysis for BSF densities without any assumptions, BSF number densities (area densities) were also estimated and were of the order of $\approx 9\times10^7 cm^{-2}$ with a corresponding PD density of $\approx 1.8\times10^8 cm^{-2}$.

❖The TD density and the BSF number densities for an m-plane $In_{0.04}Ga_{0.96}N$/GaN MQW structure were found to be $2.5\pm0.3\times10^9 cm^{-2}$ and $\approx 9.5\times10^7 cm^{-2}$ respectively.

❖ECCI may also be applied to other materials with the wurtzite crystal structure and can be combined with other SEM based characterisation techniques such as cathodoluminescence imaging and electron beam induced current.

## References


[1] D. C. Look and J. R. Sizelove, Phys. Rev. Lett. **82**, 1237, (1999).
[2] C. Trager-Cowan. et al., Phy. Rev. B **75**, 085301 (2007).
[3] J.W. P. Hsu, M. J. Manfra, R. J. Molnar, B. Heying, and J. S. Speck, Appl. Phys. Lett. **81**, 79 (2002).
[4] B. S. Simpkins, E. T. Yu, P. Waltereit, and J. S. Speck, J. Appl. Phys. **94**, 1448 (2003).
[5] G. Naresh-Kumar et al., Phys. Rev. Lett., **108**, 135503 (2012).


## Acknowledgements


Thanks to Dr. Wang and Dr. Trampert for the HR-TEM image and Jochen Bruckbauer for production of graphs and some of the images. Technical assistance from David Clark is highly appreciated.

**This work was supported by the EU project no. PITN-GA-2008-213238 (RAINBOW) and EPSRC grant no. EP/J015792/1**